water

MDPI

Article

On *Escherichia coli* Resistance to Fluid Shear Stress and Its Significance for Water Disinfection

Davide Vettori *, Costantino Manes, Davide Dalmazzo and Luca Ridolfi

Department of Environment, Land and Infrastructure Engineering, Politecnico di Torino, Corso Duca degli Abruzzi 24, 10129 Torino, Italy
* Correspondence: davide.vettori@polito.it

Abstract: Alternative water treatment techniques are needed to overcome the limitations of chemical disinfectants. Stemming from recent findings which point to high levels of shear stress induced by flow as the cause of microbial removal in water, we conducted systematic experiments on bacterial solutions in well-controlled hydrodynamic conditions to evaluate the effect of different levels of shear stress on the viability of *Escherichia coli*. We investigated a wide range of shear stresses (57–4240 Pa) using viscous substrates prepared by mixing a bacterial solution with thickeners (2-hydroxyethyl cellulose and/or guar gum). Substrate samples were tested for up to 60 min in a laminar shear flow at a constant temperature using a rotational rheometer equipped with a cone-plate measuring system so that the whole sampling volume was exposed to the same shear stress. Results show that, contrary to previous studies, high shear stresses (i.e., of order 10^3 Pa) do not induce inactivation or lysis of *E. coli*, even for prolonged exposure times. Stemming from our results and a thorough discussion of the literature on *E. coli* mechanical lysis and modeling cell dynamics, we infer that *E. coli* can resist high shear forces because of stress relaxation in a wide range of hydrodynamic conditions.

Keywords: *Escherichia coli*; shear stress; water disinfection

Citation: Vettori, D.; Manes, C.; Dalmazzo, D.; Ridolfi, L. On *Escherichia coli* Resistance to Fluid Shear Stress and Its Significance for Water Disinfection. *Water* **2022**, *14*, 2637. https://doi.org/10.3390/w14172637

Academic Editor: Helvi Heinonen-Tanski

Received: 29 July 2022
Accepted: 24 August 2022
Published: 26 August 2022
Corrected: 1 December 2022

1. Introduction

Drinking water treatments rely heavily on the use of chemical disinfectants and/or ultraviolet (UV) irradiation to remove pathogens and prevent outbreaks of waterborne diseases [1]. Unfortunately, when disinfectants react with natural organic matter (NOM) present in water, they form toxic disinfection by-products (DBPs). The DBPs that are formed depend on many biochemical and environmental factors and often are semi-volatile or volatile compounds such that their complete identification and classification are still a work in progress [2]. In treatment plants, a trade-off between pathogen control and DBP control is required, whereby water should meet drinking standards using the least possible quantity of disinfectant. Clearly, achieving such a goal is complex because of intrinsic variability in the biochemical characteristics of raw water used for potabilization and the strict limits imposed by the authorities (e.g., [3,4]).

Stemming from these limitations and because traditional water disinfection technologies are difficult to access in developing countries [5,6], scientific efforts have been underway to develop alternative ways to make water safe. Since the findings of Save et al. [7], hydrodynamic cavitation has been considered a promising technique for microbial inhibition and, more generally, water disinfection (e.g., [8–10]). Cavitation is a phenomenon whereby a decrease in pressure of a liquid below the saturated vapor pressure triggers the formation of bubbles [11], which then grow and collapse depending on pressure variations. Due to the high complexity of the physical and chemical processes it involves, it is not clear what the key mechanisms that govern its disinfection potential might be (see also the comprehensive reviews by Zupanc et al. [12] and Sun et al. [13]). However, several authors indicate high levels of shear stress, which can easily exceed 1000 Pa [14,15], associated

with microjets forming after bubble bursting as (one of) the governing mechanisms of water disinfection in hydrodynamic cavitation (e.g., [16]). This view is supported by recent findings that *E. coli* is more sensitive to shear strain rate than to cavitation [17].

This key role played by shear stress in water disinfection is likely akin to the 'shear sensitivity' phenomenon reported in bioreactors, wherein excessive mixing can reduce microbial metabolism, decrease reactor yield, or even cause microbe inhibition and lysis [18,19]. Turbulence is already used to optimize the performance of water treatments by means of better mixing (e.g., [20]) and can be exploited to reduce membrane fouling [21]. In addition, from a biological point of view, the hydrodynamic conditions of a fluid exert a considerable influence on microbial growth and viability [22,23], with turbulence modulating the nutrient uptake [24] at a microbial scale and affecting the community dynamics [25,26]. Therefore, the identification of specific hydrodynamic conditions that can cause microbial inhibition is a key step toward the development of water treatment techniques free from disinfectants.

Unfortunately, a common feature of many previous studies is that the hydrodynamic conditions are complex, and a corresponding stress status cannot be described by a simple parameter. Therefore, it is difficult to verify a causality between the conditions and the microbial viability. Only a few studies have tried to unravel the problem by isolating the effect of shear stress from the entanglement of mechanisms involved. Lange et al. [27] reported critical values of semi-instantaneous shear stress for *Escherichia coli* obtained from experiments in a Poiseuille flow followed by a jet and an impact on a flask. Two critical values of shear stress were found: 1250 Pa for cell damage, with a consequent decrease in viability, and 1810 Pa for cell lysis. Chan et al. [28] performed experiments with *E. coli* in a similar setup with maximum shear stresses between 4 and 11 $\times$ 10^3 Pa. They reported that cell damage is proportional to shear stress. They identified a governing parameter in the product of average shear rate and treatment time $\dot{\gamma}T$ (equivalently, the product of average shear stress and treatment time $\tau_{avg}T$). A 10% loss in cell viability was found for $\dot{\gamma}T = 10^4$ and $\tau_{avg}T = 65$ Pa s. Other studies with multiple treatment mechanisms concluded that high shear stress causes loss of viability in *E. coli* [17,29]. The thresholds reported by Lange et al. [27] and Chan et al. [28] are orders of magnitude lower than the typical values used in a French press for releasing proteins from bacterial cells (e.g., [30,31]), wherein pressures up to 100 MPa are achieved.

The literature provides an inconsistent picture of the effect of shear stress on microbe viability for two main reasons: (i) the hydrodynamic conditions are rarely well controlled throughout the whole experimental procedure; and (ii) in turbulent flows, bulk estimates of mechanical stresses do not reflect what microbes are actually exposed to (i.e., microbes are exposed to time-varying shear stresses). Hence these estimates should be considered just as an approximate proxy for describing loss of viability. As a result, it is difficult to prove that any microbial inhibition is caused by specific mechanisms considered in the study and to define some critical values of mechanical stresses. To shed light on this issue, in the present study, the effect of shear stress is truly isolated, differently from many previous works, by testing bacterial suspensions in a controlled laminar shear flow. In more detail, we assess the effect of different levels of shear stress on *E. coli* viability.

2. Materials and Methods

2.1. Experimental Setup

To guarantee maximum control over the flow conditions, tests were conducted with a modular compact rheometer (MCR 301, Anton Paar GmbH, Graz, Austria) that provides accurate measurements of the shear stress in the fluid being tested and is equipped with an EC motor and a Peltier system for sample temperature control (precision up to 0.01 °C). As target values of shear stress, we considered the critical values reported in Lange et al. [27] for the inhibition and mechanical lysis of *E. coli*, namely 1250 Pa and 1810 Pa, respectively. We used thickeners to enhance the viscosity of the bacterial suspensions and, thus, guarantee a laminar flow regime so that the flow properties are completely known. For the experiments,

a cone-plate measuring system was installed on the rheometer: the cone (top-part) is mobile and rotates at a selected speed in such a way as to exert a shear rate to the fluid; the plate (bottom-part) is fixed. Due to the small angle of the cone, in the cone-plate geometry, the shear rate is constant throughout the flow domain. When set into motion, the fluid in-between the shallow cone and the plate replicates a Couette flow, assuring that the stress is homogenous across the sample. Because both the gap between the cone and the plate and the velocity of fluid particles in contact with the rotating cone increase linearly as we move out of the center towards the edge of the measuring system, the shear stress τ in the flow is independent of the radial distance and can be calculated as:

$$\tau = \frac{3M}{2\pi R^3}, \quad (1)$$

where M is the torque, and R is the radius of the cone-plate measuring system.

In more detail, tests were conducted at a constant temperature (5 °C or 10 °C) using two cone-plate systems depending on the viscosity of the substrate: one with R = 24.98 mm (referred to as CP50), the other with R = 12.49 mm (referred to as CP25). In both cases, the cone truncation, which corresponds to the minimum distance between the cone and the plate during the tests, was equal to 0.05 mm and the cone angle was approximately 1°. The volume of the test sample was about 2 mL for the CP50 and 0.3 mL for the CP25.

2.2. Substrate Preparation

As thickeners, we employed 2-hydroxyethyl cellulose (HEC), a long-chain polymer produced from cellulose with an average molecular weight of 1.3×10^6 (Sigma-Aldrich, St. Louis, MO, USA, product number 434981) that has been used by Atis et al. [32] for investigating the growth dynamics of *S. cerevisiae* on an extremely viscous substrate and guar gum, a polysaccharide extracted from guar seeds. With the addition of 4.8% *w/v* of HEC or guar gum to the bacterial suspension at 10 °C, we were able to achieve a maximum viscosity of 12 Pa s at shear rate $\dot{\gamma}$ = 100 s^{-1} (corresponding to shear stress over 1000 Pa) and 61.5 Pa s at $\dot{\gamma}$ = 10 s^{-1} (corresponding to shear stress over 600 Pa), respectively. To boost the viscosity of the substrate and reach the values of shear stress (τ) never achieved previously, we combined HEC and guar gum. This way, the maximum viscosity measured was 850 Pa s at $\dot{\gamma} = 5\ s^{-1}$ (corresponding to τ = 4240 Pa) for the case with 7.5% *w/v* HEC and guar gum at 5 °C. We verified with dedicated statistical analysis that substrates with concentrations of HEC and guar gum as high as 7.5% *w/v* were not toxic for *E. coli*. It is worth noting that many resultant substrates showed a thixotropic behavior; their viscosity decreased with time when exposed to a steady shear rate (Figure 1).

For substrate preparation, a known quantity of thickener(s) previously dry-blended was added to the bacterial suspension. At the same time, the latter was being mixed with an overhead stirrer equipped with a two-blade impeller. The solution was agitated in a beaker at 100–200 rpm until it showed homogenous properties; this process took between 1 and 2 h, depending on the ambient temperature. All solutions were prepared, and solvent and solutes were weighed so that 100 mL of the substrate was obtained.

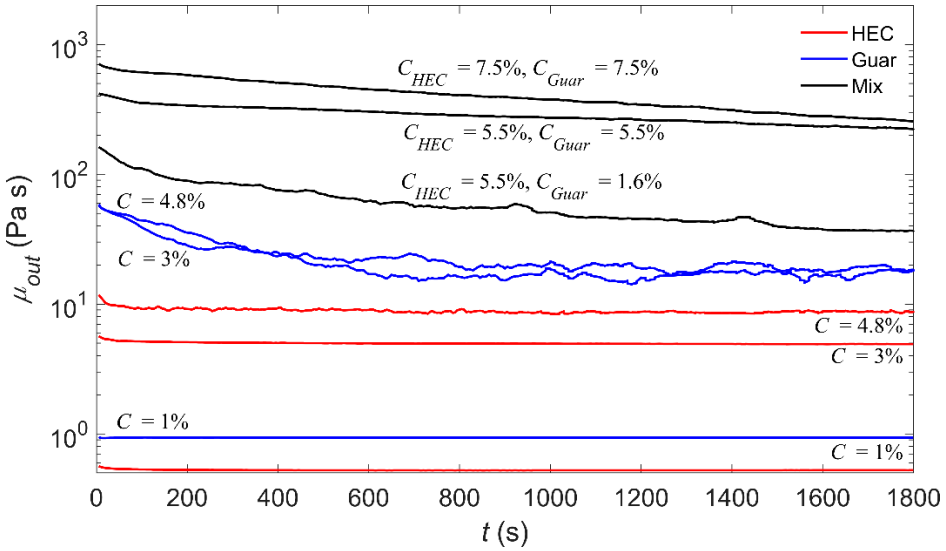

Figure 1. Variation in time of substrate viscosity during rheometer tests. Next to each curve, the concentration of thickener(s) in % *w/v* is reported. Substrates whose viscosity exceeded about 10 Pa s were strongly thixotropic.

2.3. Experimental Procedure

Bacterial suspensions were prepared the same day of the experiments rehydrating pellets of *E. coli* (ATCC® 8739™, Epower, Microbiologics, St. Cloud, MN, USA) at a known concentration for 30 min at 34–38 °C using a peptone saline solution prepared with Maximum Recovery Diluent (Millipore®). After the suspension was prepared, the bacteria concentration (C_{susp}) of the suspension was quantified with a Colilert Quanti-Tray 2000 assay (IDEXX) according to the standard procedures [33]; C_{susp} was used as a reference value to assess the effect of substrate (and substrate preparation) on *E. coli* viability. Colilert is widely used in the water research community for the assessment of the bacteriological quality of water (e.g., [34–37]). The same assay was performed to determine the bacteria concentration in all the samples prepared from the substrate, both control samples (C_0) and test samples (C). Preparation of bacterial suspensions and microbiological analysis were conducted at the Research Centre of SMAT (water utility company based in Turin).

After preparation with the bacteria suspension, the substrate was stored at fridge temperature (4 °C). For the experiments, a substrate bead was removed from the beaker with a putty knife and placed on the center of the rheometer's plate (Figure 2a,c). From the same bead, a small quantity was extracted and inserted into a flask to be used as a control sample. This quantity, not exposed to shear stress treatment and equal to 0.1 mL for tests with CP50 and 0.02 mL for tests with CP25, was kept in a fridge for the duration of the tests. The remaining part of the bead was used in the experiment as the test sample. From each substrate, up to 9 beads, depending on the substrate viscosity, were extracted and tested.

After the substrate bead was placed on the bottom plate (Figure 2a,c), it was homogenously distributed throughout the surface by slowly lowering the cone until it reached the testing position. Namely, the cone tip was 0.05 mm away from the plate. Before starting the tests, the excess substrate expelled from the measuring system due to the cone being lowered was manually removed with a putty knife. Each test was initialized, applying a low shear rate for 1 min to set the test sample into motion and avoid strong accelerations. Then the target shear rate was reached and maintained for a time between 5 and 60 min, thus ensuring a steady laminar flow. We verified that all tests were performed in a laminar regime by estimating the Reynolds number ($Re = 2\pi R\dot{\gamma}h\rho/\mu_{end}$, where R is the radius of the cone-plate measuring system, $\dot{\gamma}$ is the shear rate, h is the gap between cone and plate, ρ is the substrate mass density and μ_{end} is the substrate dynamic viscosity at the end of the test, at its minimum) on the edge of the cone-plate system (where the linear velocity

and the gap are at their maximum) and found that $Re < 30$ for all cases (see Supplementary Information 'Dataset_1'). Because the substrates tested are extremely viscous and the distance between the plate and cone very small (less than 0.5 mm at the edge of the measuring system), for the purpose of data collection, it is safe to consider that the flow was in a steady state. Indeed, the timescale (t_s) for relaxation to steady state, which scales as $t_s \sim h^2/\nu$, where h is the maximum flow height, and ν is the kinematic viscosity of the fluid [38], is on the order of milliseconds or lower for all tests considered herein.

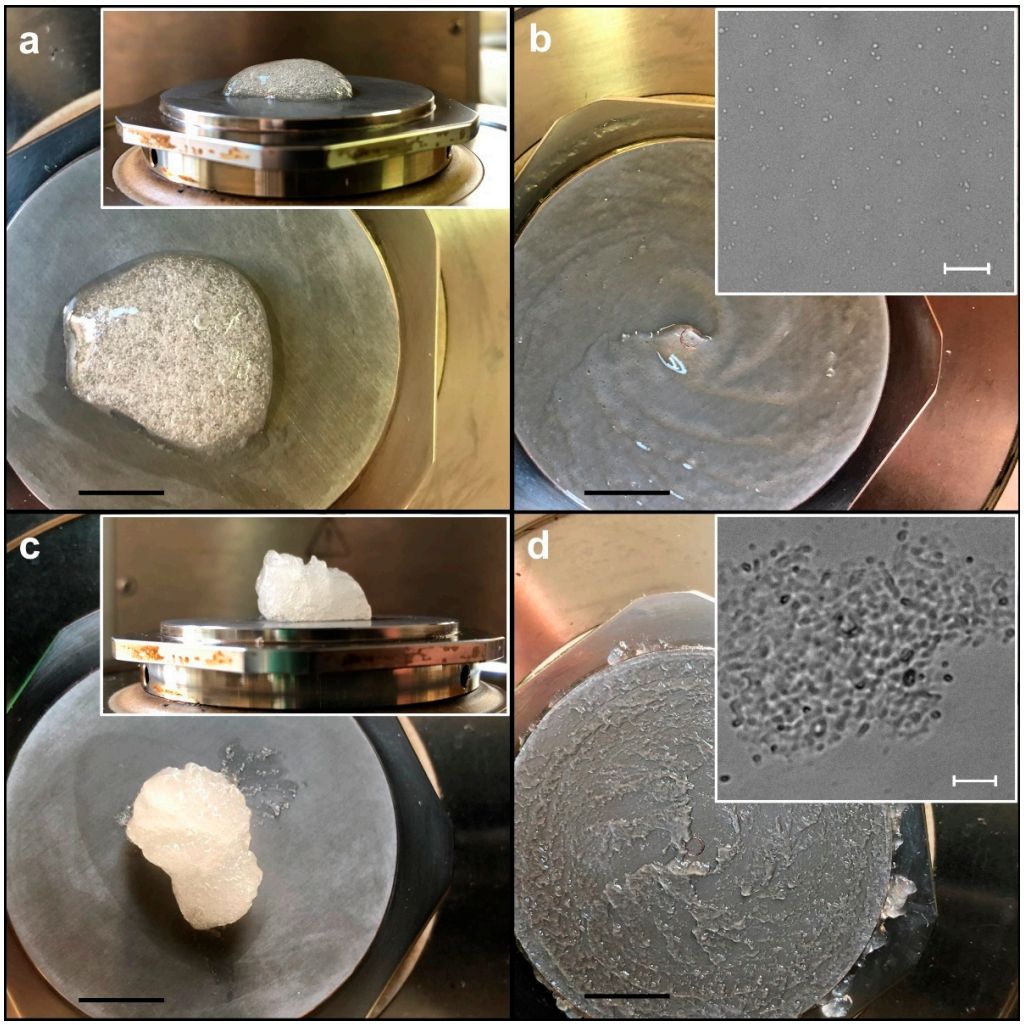

Figure 2. Top view of substrate beads on the rheometer bottom plate. Substrate with 3% *w/v* HEC before (**a**) and after (**b**) experiment; substrate with 5% *w/v* HEC and 1.6% *w/v* guar gum before (**c**) and after (**d**) experiment (the black scale bars are 10 mm). In (**a**,**c**), the insets are side-views of the substrate bead in the respective images. In (**b**,**d**), the insets show *E. coli* cells after the experiment in the respective substrate sample; images were taken with an optical microscope (white scale bars are 10 µm). The spatial distribution of cells agrees with Atis et al. [32] and Dufrêne and Persat [39], i.e., colonies are more compact when the substrate is highly viscous.

During the tests, measurements of torque M were acquired every 5 s by means of dedicated software (RheoPlus, v.3.0). From these, the shear stress Equation (1) and the dynamic viscosity were calculated at the same time instants. Note that some of the substrate bead being tested was lost as the testing volume tends to slowly empty. For this reason, the torque (and dynamic viscosity and shear stress) measured displays a considerable reduction in time (Figure 1). After reaching the prescribed exposure time (Figure 2b,d), the test sample was removed from the plate, and the same quantity used for the control sample was inserted in a flask. Both the control and test samples were then diluted with

ultra-pure water within their flask to obtain a final volume of 100 mL, which is required for conducting Colilert analysis. The flasks were shaken repeatedly to facilitate substrate dissolution in water and stored in a fridge for up to 24 h prior to determining bacterial concentrations in control samples (C_0) and test samples (C). At the end of each test, all relevant equipment was sterilized with a 0.1% H_2O_2 w/w solution and repeatedly rinsed with ultra-pure water prior to new use.

2.4. Experimental Procedure

Since the bacterial removal efficiency was not normally distributed (Kolmogorov–Smirnov test, $p << 0.01$), to assess the potential correlations between bacterial removal efficiency and all parameters of interest, we used robust linear regression models with a bisquare weight function to reduce the weight of outliers. The significance of correlations was tested with Student's t-tests setting $\alpha = 0.05$. For all hydrodynamic parameters that were used as predictors of the treatment, the removal efficiency was set to zero when the predictor was null. Namely, the intercept of the regressions was forced to zero. For all models, the adequacy of fit was checked with relevant residual plots. The 95% confidence interval for the bacterial removal efficiency was calculated from the 95% confidence interval for the Colilert Quanti-Tray 2000 assay [33] using uncertainty propagation [40]. All data post-processing and statistical analysis were conducted with MATLAB R2019b®.

3. Results

A total of 25 substrates with a concentration of thickeners varying from 1% *w/v* 2-hydroxyethyl cellulose (HEC) or guar gum (least viscous case) to 7.5% *w/v* HEC and guar gum (most viscous case) were prepared by mixing the thickeners with a bacterial suspension with concentration (C_{susp}) between 2.1×10^5 and 6.5×10^6 CFU/100mL. The influence of the substrate preparation procedure on bacterial viability was quantified by comparing the bacterial concentration (C_0) in substrate control samples with the concentration in the bacterial suspension (C_{susp}) used for substrate preparation (see Section 2.3 for details). Throughout the 25 substrates prepared, an average 26% reduction in bacterial viability was recorded, and the bacterial concentration ranged between 5×10^4 and 5.6×10^6 CFU/100 mL. From these substrates, 107 test samples were obtained and used in the experiments wherein they were exposed to shear stress treatments in a laminar Couette flow with shear stress between 57 and 4240 Pa (see Supplementary Information 'Dataset_1' for further details). We assessed whether there was a correlation between the bacterial removal efficiency (defined as $v_r = 1 - C/C_0$, where C is the bacterial concentration in the test sample and C_0 is the bacterial concentration in the control sample) due to the treatment and the shear stress exerted by the flow using the following parameters: the level of shear stress τ (Figure 3a), the time wherein the critical values $\tau_{crit,L}$ of shear stress identified by Lange et al. [27] are exceeded $\Delta t = t(\tau > \tau_{crit,L})$ (Figure 3b), and the product of average shear stress and treatment time $\tau_{avg}T$ (Figure 3c). During experiments, a constant level of shear rate was imposed on the test sample, but because of the thixotropic nature of the substrate and the loss of substrate during the test, probably due to inertial effects and edge fracture [41], the shear stress exerted varied in time in most cases. For this reason, in the analysis, we considered both the maximum shear stress τ_{max} (usually achieved at the beginning of the test) and the time-average shear stress τ_{avg} (Figure 3a). The product of average shear rate and treatment time $\dot{\gamma}T$ (proposed by Chan et al. [28]) was not employed because of the limited number of shear rate values used for the experiments (see Supplementary Information 'Dataset_1').

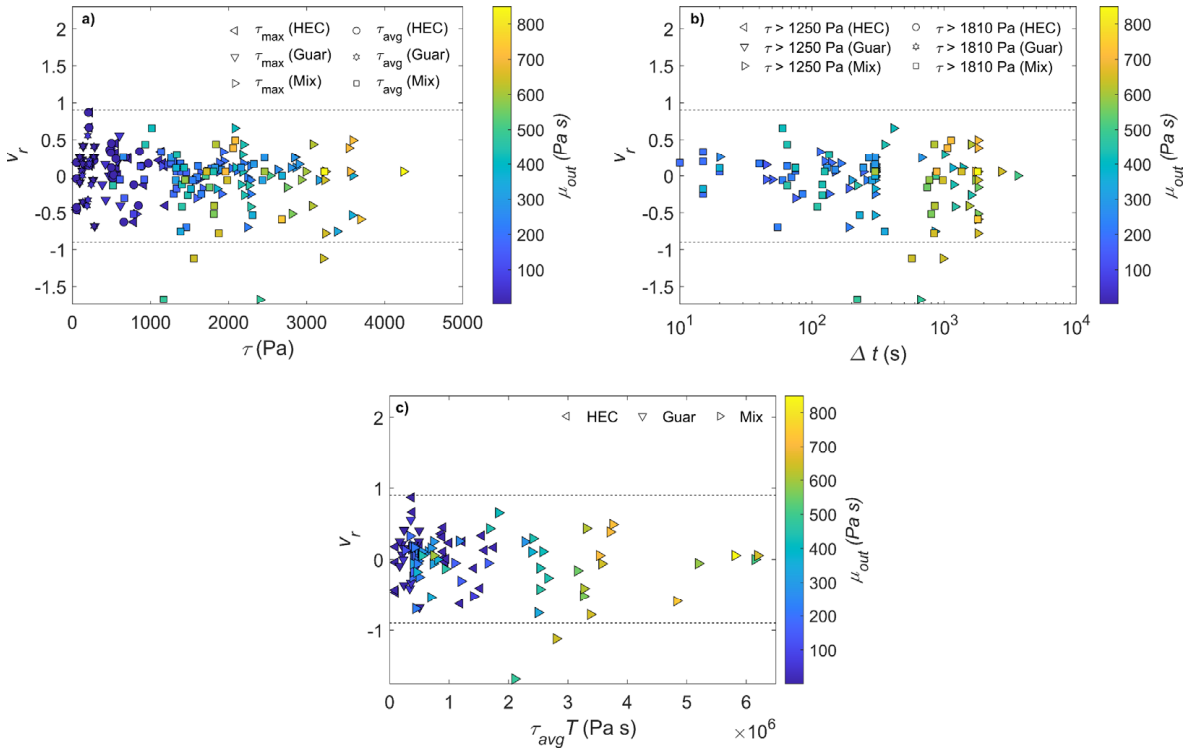

Figure 3. Bacterial removal efficiency as a function of (**a**) the maximum and time-averaged shear stress; (**b**) the time during which the shear stress exceeded the critical values reported in Lange et al. [27] for cell damage and lysis; (**c**) the product of average shear stress and treatment time. The horizontal dashed lines represent the 95% confidence interval for the removal efficiency calculated from the confidence intervals for the Colilert Quanti-Tray 2000 assay. The color bars report the viscosity of the substrates.

Figure 3a–c displays the bacterial removal efficiency as a function of all hydrodynamic parameters considered. Note that for the times during which the critical values proposed by Lange et al. [27] were exceeded, namely $\Delta t_1 = t(\tau > 1250 \text{ Pa})$ and $\Delta t_2 = t(\tau > 1810 \text{ Pa})$, the number of samples used for the statistical test (and displayed in Figure 3b) is reduced because the critical values of τ were not exceeded in all tests. Student's t-test does not reject the hypothesis that the mean bacterial removal efficiency across all tests is null (t_s (106) = 0.1, p = 0.92, where t_s is the t-test parameter reported with the degrees of freedom). There is no significant correlation between the removal efficiency and the parameters, in more detail: for τ_{max} R^2 = 0.33 and p = 0.78 (t_s (106) = 0.28); for τ_{avg} R^2 = 0.33 and p = 0.76 (t_s (106) = 0.31); for $\tau_{avg}T$ R^2 = 0.33 and p = 0.89 (t_s (106) = 0.14); for $\Delta t_1 = t(\tau > 1250 \text{ Pa})$ R^2 = 0.29 and p = 0.74 (t_s (59) = −0.33); and for $\Delta t_2 = t(\tau > 1810 \text{ Pa})$ R^2 = 0.33 and p = 0.75 (t_s (50) = −0.32). Moreover, we verified that the removal efficiency was not significantly correlated with the bacterial concentration at the beginning of the test (R^2 = 0.03 and t_s (105) = 0.87, p = 0.39). It is also worth noting that the removal efficiency is independent of the thickener(s) being used or the viscosity μ_{out} of the substrates.

4. Discussion

4.1. Comparison with Previous Studies on E.coli Lysis

Independently of the parameter with which we characterize the mechanical forcing induced by the flow on the cells, our results indicate that bacteria viability is not affected by the shear stress treatments applied in the experiments. This finding is unexpected and in contrast with the (rather limited) experimental data available in the literature. In more detail, Lange et al. [27] reported a loss in viability up to 80% and 20% when *E. coli* cell suspensions were exposed to maximum shear stress of 1810 Pa for 30 ms and 1250 Pa for

50 ms, respectively. The data collected during the present study showed no loss of viability for values of shear stress up to over 4200 Pa and exerted for many seconds (up to 3600 s). Furthermore, it is worth noting that the values of τ_{avg} calculated herein are likely to be biased low because of the loss of substrate that could happen during the tests. In their experimental work, Chan et al. [28] also considered the contribution of treatment time to the loss of viability and described a viability loss of 10% for $\dot{\gamma}T = 10^4$ and $\tau_{avg}T = 65$ Pa s. Even though $\dot{\gamma}T$ and $\tau_{avg}T$ in our test are up to 10^5 and 10^6 Pa s, respectively, there is no significant correlation between bacteria viability and the parameters proposed by Chan et al. [28].

It is possible that the discrepancy between our results and those of previous studies may arise because, in the present study, *E. coli* were re-hydrated from pellets, while both Lange et al. [27] and Chan et al. [28] cultured the bacteria in rich media. If this were the case, we would expect the bacteria used in the present study to be less resistant to mechanical stresses, as evidenced by studies on osmotic treatments wherein fast rehydration can induce cell lysis (e.g., [42]), but the results demonstrate the opposite. Alternatively, this discrepancy may be due to methodological limitations in the present work that make the bacteria concentration very noisy and do not allow for identifying potential trends in the data. In particular, this issue may arise because of: (1) the higher relative error associated with the Colilert assay [33] compared to the counting methods used in the literature; and/or (2) a low homogenization of the substrate caused by the way in which it was prepared, even though this is unlikely because the average coefficient of variation of bacterial concentration in control samples across all substrates is equal to 18%. Notwithstanding these limitations, the values of shear stress (and also of $\dot{\gamma}T$ and $\tau_{avg}T$) achieved herein are so much higher than the critical values reported in the literature that we would expect a considerable reduction in the concentration of *E. coli* that becomes visible despite the relative error associated with the Colilert Quanti-Tray 2000 assay (Figure 3a–c). Since this is not the case, we now consider the maximum stresses *E. coli* cells can bear before lysis to explain why we did not observe a significant loss of viability of *E. coli* in our experiments.

4.2. Estimating Flow-Induced Stress for E. coli Lysis

Gram-negative bacteria, such as *E. coli*, are characterized by a composite cell envelope that surrounds the cell, gives it mechanical stability, and controls its shape [43]. A rough estimate of the hydrodynamic stresses required to induce bacterial cell lysis could be obtained from values of tension at breakage of the bulk cell envelope. While we are not aware of any study reporting such values, two recent studies estimated the tension at breakage for the inner membrane of *E. coli* as 79 mN/m [44] and a generic lipid bilayer as 45 mN/m [45] via molecular dynamics simulations. Assuming that these estimates can be applied to the whole envelope and considering the thickness of the cell envelope layers reported in the literature [46–48], the flow-induced stress required to break the cell envelope is on the order of 10^6–10^7 Pa. This range of values is close to that of the maximum peak pressure (10^8 Pa) to which *E. coli* cells survived in shock experiments conducted to test the hypothesis of panspermia [49] and to the pressure applied in a French press to extract intracellular proteins [30,31]. Hence, simple considerations on flow-induced stresses based on the mechanical properties at breakage of *E. coli* cell envelopes may explain our results but clash with the findings of previous studies, where values of shear stress reported for cell lysis are several orders of magnitude lower (on the order of 10^3 Pa).

4.3. On Modelling Cell Deformation and Dynamics

We expect that for bacterial cells to undergo lysis, it is not necessary to reach the large stress required to break the cell envelope (i.e., on the order of 10^6–10^8 Pa). However, the cell envelope may experience mechanical fatigue and break after repeated events, causing sublytic damage, a mechanism similar to what was reported for RBCs [50]. To examine this hypothesis, we now model cell deformation and dynamics using simple models developed for elastic capsules and vesicles (see comprehensive review by Barthes-Biesel [51]), which

are made of lipid bilayers enclosing an internal liquid; these nearly spherical particles replicate the structure of microbial cells. It is generally accepted that vesicles (and RBCs) show three main dynamic states in shear flows: at low shear, they tumble like quasi-solid particles. As the shear increases, they rotate and show periodic deformations (so-called swinging or trembling state), and at high shear, they assume an ellipsoidal shape and rotate around the inner fluid (so-called tank-treading state) [50,51]. Through dimensional considerations, the deformation of elastic capsules can be described by three dimensionless parameters, the viscosity ratio λ, the capillary number Ca, and the wall to bulk viscosity ratio η:

$$\lambda = \frac{\mu_{in}}{\mu_{out}}, \tag{2}$$

$$Ca = \frac{\mu_{out}\dot{\gamma}r}{E_b b}, \tag{3}$$

$$\eta = \frac{\mu_{wall}}{\mu_{out}r}, \tag{4}$$

where μ_{in}, μ_{out}, and μ_{wall} indicate the dynamic viscosity of the cell inner fluid, of the substrate (outer fluid), and the cell envelope, $\dot{\gamma}$ is the shear rate, r is the cell equivalent spherical radius, b and E_b are the cell envelope thickness and elastic modulus, respectively [51,52]. To describe the dynamics of quasi-spherical vesicles, Lebedev et al. [53] introduced a pair of dimensionless parameters, obtained by solving the dynamical equation for membrane displacement, which are used to build a 2D phase diagram of vesicle dynamical states (of the type displayed in Figure 4). Bearing in mind that *E. coli* cells are not perfectly spherical and the cell envelope includes a cell wall (not accounted for in the model), we use these results as a first approximation. For a simple shear flow, these parameters have been introduced by Deschamps et al. [54], and they read:

$$S = \frac{7\pi}{3\sqrt{3}} \frac{\mu_{out}\dot{\gamma}r^3}{k\Delta}, \tag{5}$$

$$\Lambda = \frac{4}{\sqrt{30\pi}} \left(1 + \frac{23}{32}\lambda\right) \sqrt{\Delta}, \tag{6}$$

where k is the cell envelope bending modulus and Δ is the cell excess area (defined as $\Delta = A/r^2 - 4\pi$, where A is the cell surface area). To estimate the values of these dimensionless parameters (Equations (2)–(6)) in the experiments presented herein, we make use of bulk morphological characteristics and mechanical properties of the *E. coli* cell envelope reported in the relevant literature (see Table 1). From these, the following quantities, used in Equations (2)–(6), can be defined: cell envelope thickness $b = b_o + b_i + b_p$, and cell envelope bending modulus $k = k_a b^2$. To calculate k, the area expansion modulus k_a of lipid membranes was applied to the whole cell envelope as a simplification because the area expansion modulus of the peptidoglycan is negligible at small extensions [44]. It is worth noting that if a different bending modulus were used, for the purposes of our modeling this would imply a variation only in the parameter S (Equation (5)), while Λ would be unaffected.

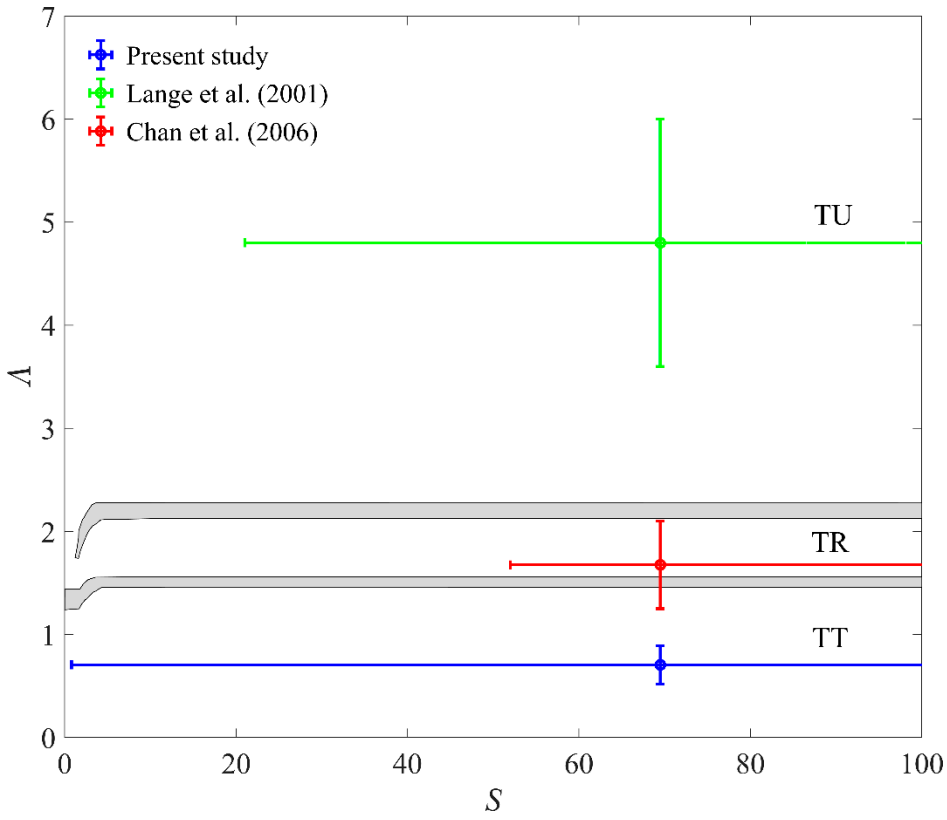

Figure 4. Phase diagram of the vesicle dynamical state with data from Lange et al. [27], Chan et al. [28] and Deschamps et al. [54]. TU stands for tumbling state, TR for trembling state, and TT for tank-treading state. Grey bands are the transition regions identified experimentally by Deschamps et al. [54]. The ranges of values of S and Λ for this study and other relevant studies with *E. coli* are reported with bars (note that the diagram is cut-off at $S = 100$ for graphical reasons).

Table 1. Values of morphological and mechanical parameters of cell envelopes for *E. coli* (unless differently specified) from the literature. According to the literature [55] *E. coli* cells can be represented by end-capped rods/cylinders.

Parameter	Symbol	Range of Values	Units	Source	Notes
Thickness of outer membrane	b_o	3.7	nm	[47]	-
Thickness of inner membrane	b_i	7	nm	[48]	-
Thickness of peptidoglycan	b_p	<4	nm	[46]	Only maximum value is reported
Major axis	a_1	1–4	µm	[55]	-
Minor axis	a_2	0.4–0.8	µm	[55]	-
Cytoplasm viscosity	μ_{in}	9.7	mPa s	[56]	Used as the cell inner fluid viscosity
Cell envelope viscosity	μ_{wall}	30	nPa s m	[57]	For generic mixed lipid membranes
Elastic modulus of cell envelope	E_b	2–31	MPa	[58,59]	From atomic force microscopy measurements
Area expansion modulus of lipid membranes	k_a	240	mN/m	[44]	From experiments with a Langmuir trough
Area expansion modulus of cell wall	$k_a{}^{cw}$	30–500	mN/m	[44]	From molecular dynamics simulations

Concerning experimental parameters, the shear rate was calculated as the average value throughout the test (note that it was kept constant during the tests), and two values of substrate viscosity were considered: the maximum value achieved at the beginning of the tests, and the minimum value reached at the end of the tests (this variation is due to the thixotropic behavior of the substrate and loss of substrate during the test, see the evolution of viscosity in Figure 1). The ranges of values for the dimensionless parameters depended on the substrate viscosity used and are reported in Table 2. While the deformation at low values of λ should not differ significantly from that for λ = O(1) [51] (but no previous studies report values as low as in the present study), *Ca* in our experiments is too low to induce large deformation and, potentially, cell lysis [52]; but this is true for previous studies as well (see estimates for previous studies in Table 2). Values of $\eta < 1$ have not been considered in the literature, so it is impossible to evaluate the potential effect of this parameter on the results.

Table 2. Values of dimensionless parameters describing vesicle deformation and dynamics in the present study and in previous studies investigating the effect of shear stress on *E. coli* (note that the large variation in values is associated with the high variability of cell mechanical parameters).

	Present Study with Max μ_{out} (Beginning of Tests)	**Present Study with min μ_{out} (End of Tests)**	**Lange et al. [27]**	**Chan et al. [28]**
λ	1×10^{-5}–1.7×10^{-2}	2×10^{-5}–1.9×10^{-2}	8.2	1.9
Ca	3×10^{-5}–1×10^{-1}	3×10^{-5}–6×10^{-2}	7×10^{-4}–3×10^{-2}	2×10^{-3}–8×10^{-2}
η	5×10^{-5}–2×10^{-1}	8×10^{-5}–2.1×10^{-1}	37–94	8.8–22
S	0.9–240	0.8–387	21–118	52–296
Λ	0.52–0.89	0.52–0.89	3.6–6	1.25–2.1

We now shift the focus of our discussion to the cell dynamics as predicted by the experiment-based phase diagram presented by Deschamps et al. [54] (see Figure 4). In the tests presented herein, mainly due to the low values of Λ, cells are in the tank-treading (TT in Figure 4) state, where stress relaxation occurs via rotation [60], likely preventing cell lysis regardless of the shear applied. The conditions tested by Lange et al. [27] fall in the tumbling state (TU in Figure 4) of the phase diagram, in which cells are exposed to low shear forces and experience small deformations. Interestingly, the tests described in Chan et al. [28] fall within the trembling state (TR in Figure 4), in which cells undergo large deformations that involve third and higher-order harmonics. It is possible that relatively long exposure to the trembling state could cause cell lysis via a sort of mechanical fatigue, which may be the case for the experiments conducted by Chan et al. [28]. Unfortunately, no models of vesicle or elastic capsule breakup are available in the literature. Therefore this speculation would need to be supported by experimental data that are currently not available.

4.4. Reconciling with the Literature: The Role of Turbulence

Accounting for cell dynamical states cannot explain the discrepancy between the results of our experiments and those reported in the literature in its entirety. Therefore, we infer that this discrepancy can only be due to the different experimental conditions. In the present study, we isolated the effect of shear stress from any other important mechanism by performing experiments in a laminar regime. It is our view that in previous experimental studies, the hydrodynamic conditions were not as well-controlled and, hence, the microbial suspension was actually exposed to peak levels of shear stress much higher than those reported, possibly due to contractions/expansions or jets and strong turbulence whose effects have not been accounted for appropriately.

Thus, it is highly likely that the values of shear stress reported in the relevant literature are spatial-temporal averages at best and, as such, do not represent the stresses microbes were effectively exposed to. Indeed, in a strong turbulent flow, mechanical stresses vary

randomly (in a statistical sense) in magnitude and direction, and their instantaneous values well exceed their time averages [61]. We hypothesize that small-scale turbulence may cause large deformation to microbes comparable with those reported for vesicles in the trembling state. These large deformations, even though local in nature, can lead to considerable variations in cell shape and, hence, lead to a fatigue of the cell envelope that would eventually cause cell lysis at levels of stress much lower than the critical values obtained from simple mechanical considerations (see Section 4.1). It is also likely that by causing mechanical fatigue, turbulence would speed up the diffusion of oxidants through the cell envelope, thus making chemical disinfectants more effective.

5. Conclusions

Recent studies suggest that high levels of shear stress induced by the flow can reduce microbial viability. To identify a threshold of shear stress for inhibition or lysis of bacteria, in the present study, we exposed *E. coli* to different levels of shear stress in a steady laminar flow and monitored its viability. Levels of shear stress over 4000 Pa, never reached previously, were achieved using substrates prepared with thickeners that did not impact *E. coli* viability. Our results indicate that *E. coli* viability was not correlated with the values of shear stress or the product of shear stress and treatment time, implying that a high level of shear stress is not sufficient to induce inhibition.

Turbulence governs the dynamics of microbes at a community scale, and there are numerous observations of flow shear affecting the dynamics of bacterial communities [25,26]. In a similar fashion, it has been proposed that small-scale turbulence can modulate the nutrient uptake and growth of microbes [24]. Stemming from the results presented herein, we take a step forward and propose that intense turbulence may be used as a tool for microbial inactivation/lysis. Direct observations of turbulence's ability to inactivate microbes are still lacking. However, if our working hypothesis is confirmed, it will represent a game changer for water disinfection, allowing the development of novel low-cost water disinfection techniques.

Supplementary Materials: The following supporting information can be downloaded at: https://www.mdpi.com/article/10.3390/w14172637/s1; Data collected used in the present work.

Author Contributions: Conceptualization, D.V., C.M. and L.R.; methodology, D.V. and D.D.; software, D.V.; validation, D.V.; formal analysis, D.V.; investigation, D.V. and D.D.; resources, L.R. and D.D.; data curation, D.V.; writing—original draft preparation, D.V.; writing—review and editing, D.V., C.M., L.R. and D.D.; visualization, D.V.; supervision, C.M. and L.R.; project administration, D.V. and L.R.; funding acquisition, L.R. All authors have read and agreed to the published version of the manuscript.

Funding: Funding for this work was provided by the European Union through Regione Piemonte (Project BioEnPro4To POR FESR 2014/2020). The APC was funded by the European Union through Regione Piemonte (Project BioEnPro4To POR FESR 2014/2020).

Institutional Review Board Statement: Not applicable.

Informed Consent Statement: Not applicable.

Data Availability Statement: Data are available as Supplementary Material to the article.

Acknowledgments: The authors would like to thank Giada Gregucci (SMAT) for the preparation of the bacterial suspensions and the conduction of Colilert Quanti-Tray 2000 assays, Riccardo Rabezzana for technical support with the rheometer and Francesca Frascella for shooting microscope photos.

Conflicts of Interest: The authors declare no conflict of interest. The funders had no role in the design of the study; in the collection, analyses, or interpretation of data; in the writing of the manuscript; or in the decision to publish the results.

References

1. White, G.C. *Handbook of Chlorination and Alternative Disinfectants*; Wiley: New York, NY, USA, 2010; ISBN 0470180986.
2. Li, X.-F.; Mitch, W.A. Drinking Water Disinfection Byproducts (DBPs) and Human Health Effects: Multidisciplinary Challenges and Opportunities. *Environ. Sci. Technol.* **2018**, *52*, 1681–1689. [CrossRef] [PubMed]
3. EU. Directive (EU) 2020/2184 of The European Parliament and of the Council of 16 December 2020 on the Quality of Water Intended for Human Consumption (Recast). *Off. J. Eur. Union* **2020**, *L 435/1*, 1–62.
4. U.S. Environmental Protection Agency National Primary Drinking Water Regulations. Available online: https://www.epa.gov/ground-water-and-drinking-water/national-primary-drinking-water-regulations (accessed on 13 October 2021).
5. World Health Organization; The United Nations Children's Fund. *Progress on Drinking Water, Sanitation and Hygiene: 2017 Update and Sdg Baselines*; WHO: Geneva, Switzerland; UNICEF: New York, NY, USA, 2017.
6. World Bank Group. *Reducing Inequalities in Water Supply, Sanitation, and Hygiene in the Era of the Sustainable Development Goals: Synthesis Report of the WASH Poverty Diagnostic Initiative*; World Bank Group: Singapore, 2017.
7. Save, S.S.; Pandit, A.B.; Joshi, J.B. Microbial Cell Disruption: Role of Cavitation. *Chem. Eng. J. Biochem. Eng. J.* **1994**, *55*, B67–B72. [CrossRef]
8. Burzio, E.; Bersani, F.; Caridi, G.C.A.; Vesipa, R.; Ridolfi, L.; Manes, C. Water Disinfection by Orifice-Induced Hydrodynamic Cavitation. *Ultrason. Sonochem.* **2019**, *60*, 104740. [CrossRef]
9. Dular, M.; Griessler-Bulc, T.; Gutierrez-Aguirre, I.; Heath, E.; Kosjek, T.; Klemenčič, A.K.; Oder, M.; Petkovšek, M.; Rački, N.; Ravnikar, M. Use of Hydrodynamic Cavitation in (Waste) Water Treatment. *Ultrason. Sonochem.* **2016**, *29*, 577–588. [CrossRef]
10. Šarc, A.; Kosel, J.; Stopar, D.; Oder, M.; Dular, M. Removal of Bacteria *Legionella Pneumophila*, *Escherichia Coli*, and *Bacillus Subtilis* by (Super) Cavitation. *Ultrason. Sonochem.* **2018**, *42*, 228–236. [CrossRef] [PubMed]
11. Brennen, C.E. *Cavitation and Bubble Dynamics*; Cambridge University Press: Cambridge, UK, 2014; ISBN 1107644763.
12. Zupanc, M.; Pandur, Ž.; Perdih, T.S.; Stopar, D.; Petkovšek, M.; Dular, M. Effects of Cavitation on Different Microorganisms: The Current Understanding of the Mechanisms Taking Place behind the Phenomenon. A Review and Proposals for Further Research. *Ultrason. Sonochem.* **2019**, *57*, 147–165. [CrossRef] [PubMed]
13. Sun, X.; Liu, J.; Ji, L.; Wang, G.; Zhao, S.; Yoon, J.Y.; Chen, S. A Review on Hydrodynamic Cavitation Disinfection: The Current State of Knowledge. *Sci. Total Environ.* **2020**, *737*, 139606. [CrossRef]
14. Zeng, Q.; Gonzalez-Avila, S.R.; Dijkink, R.; Koukouvinis, P.; Gavaises, M.; Ohl, C.-D. Wall Shear Stress from Jetting Cavitation Bubbles. *J. Fluid Mech.* **2018**, *846*, 341–355. [CrossRef]
15. Dijkink, R.; Ohl, C.-D. Measurement of Cavitation Induced Wall Shear Stress. *Appl. Phys. Lett.* **2008**, *93*, 254107. [CrossRef]
16. Sawant, S.S.; Anil, A.C.; Krishnamurthy, V.; Gaonkar, C.; Kolwalkar, J.; Khandeparker, L.; Desai, D.; Mahulkar, A.V.; Ranade, V.V.; Pandit, A.B. Effect of Hydrodynamic Cavitation on Zooplankton: A Tool for Disinfection. *Biochem. Eng. J.* **2008**, *42*, 320–328. [CrossRef]
17. Schiffer, A.; Gardner, M.N.; Lynn, R.H.; Tagarielli, V.L. A New Apparatus to Induce Lysis of Planktonic Microbial Cells by Shock Compression, Cavitation and Spray. *R. Soc. Open Sci.* **2017**, *4*, 160939. [CrossRef] [PubMed]
18. Rikmanis, M.; Berzinš, A.; Viesturs, U. Excess Turbulence as a Cause of Turbohypobiosis in Cultivation of Microorganisms. *Cent. Eur. J. Biol.* **2007**, *2*, 481–501. [CrossRef]
19. Wang, C.; Lan, C.Q. Effects of Shear Stress on Microalgae—A Review. *Biotechnol. Adv.* **2018**, *36*, 986–1002. [CrossRef] [PubMed]
20. Chan, S.N.; Qiao, Q.S.; Lee, J.H.W.; Choi, K.W.; Huang, J.-C. Modeling of Mixing and Rapid Chlorine Demand in Sewage Disinfection with Dense Chlorine Jets. *J. Environ. Eng.* **2017**, *143*, 4017074. [CrossRef]
21. Pourbozorg, M.; Li, T.; Law, A.W.K. Effect of Turbulence on Fouling Control of Submerged Hollow Fibre Membrane Filtration. *Water Res.* **2016**, *99*, 101–111. [CrossRef]
22. Al-Homoud, A.; Hondzo, M. Enhanced Uptake of Dissolved Oxygen and Glucose by Escherichia Coli in a Turbulent Flow. *Appl. Microbiol. Biotechnol.* **2008**, *79*, 643–655. [CrossRef]
23. Hondzo, M.; Al-Homoud, A. Model Development and Verification for Mass Transport to Escherichia Coli Cells in a Turbulent Flow. *Water Resour. Res.* **2007**, *43*, 1–11. [CrossRef]
24. Hondzo, M.; Wüest, A. Do Microscopic Organisms Feel Turbulent Flows? *Environ. Sci. Technol.* **2009**, *43*, 764–768. [CrossRef]
25. Durham, W.M.; Kessler, J.O.; Stocker, R. Disruption of Vertical Motility by Shear Triggers Formation of Thin Phytoplankton Layers. *Science* **2009**, *323*, 1067–1070. [CrossRef]
26. Durham, W.M.; Climent, E.; Barry, M.; De Lillo, F.; Boffetta, G.; Cencini, M.; Stocker, R. Turbulence Drives Microscale Patches of Motile Phytoplankton. *Nat. Commun.* **2013**, *4*, 2148. [CrossRef] [PubMed]
27. Lange, H.; Taillandier, P.; Riba, J. Effect of High Shear Stress on Microbial Viability. *J. Chem. Technol. Biotechnol.* **2001**, *76*, 501–505. [CrossRef]
28. Chan, G.; Booth, A.J.; Mannweiler, K.; Hoare, M. Ultra Scale-down Studies of the Effect of Flow and Impact Conditions during E. Coli Cell Processing. *Biotechnol. Bioeng.* **2006**, *95*, 671–683. [CrossRef] [PubMed]
29. Mok, J.H.; Pyatkovskyy, T.; Yousef, A.; Sastry, S.K. Combined Effect of Shear Stress and Moderate Electric Field on the Inactivation of Escherichia Coli K12 in Apple Juice. *J. Food Eng.* **2019**, *262*, 121–130. [CrossRef]
30. Goldberg, A.L.; Swamy, K.H.S.; Chung, C.H.; Larimore, F.S. Proteases in Escherichia Coli. *Methods Enzymol.* **1981**, *80*, 680–702.
31. Balasundaram, B.; Harrison, S.T.L. Study of Physical and Biological Factors Involved in the Disruption of *E. coli* by Hydrodynamic Cavitation. *Biotechnol. Prog.* **2006**, *22*, 907–913. [CrossRef]

32. Atis, S.; Weinstein, B.T.; Murray, A.W.; Nelson, D.R. Microbial Range Expansions on Liquid Substrates. *Phys. Rev. X* **2019**, *9*, 21058. [CrossRef]
33. *ISO 9308-2*; Water Quality—Enumeration of *Escherichia coli* and Coliform Bacteria—Part 2: Most Probable Number Method. ISO: Geneva, Switzerland, 2012.
34. Vang, Ó.K.; Corfitzen, C.B.; Smith, C.; Albrechtsen, H.-J. Evaluation of ATP Measurements to Detect Microbial Ingress by Wastewater and Surface Water in Drinking Water. *Water Res.* **2014**, *64*, 309–320. [CrossRef]
35. Fricker, E.J.; Illingworth, K.S.; Fricker, C.R. Use of Two Formulations of Colilert and QuantiTray^{TM} for Assessment of the Bacteriological Quality of Water. *Water Res.* **1997**, *31*, 2495–2499. [CrossRef]
36. Hamilton, W.P.; Kim, M.; Thackston, E.L. Comparison of Commercially Available Escherichia Coli Enumeration Tests: Implications for Attaining Water Quality Standards. *Water Res.* **2005**, *39*, 4869–4878. [CrossRef]
37. Nilsen, V.; Christensen, E.; Myrmel, M.; Heistad, A. Spatio-Temporal Dynamics of Virus and Bacteria Removal in Dual-Media Contact-Filtration for Drinking Water. *Water Res.* **2019**, *156*, 9–22. [CrossRef] [PubMed]
38. Schlichting, H.; Gersten, K. *Boundary-Layer Theory*, 9th ed.; Springer: Berlin/Heidelberg, Germany, 2017; ISBN 366252919X.
39. Dufrêne, Y.F.; Persat, A. Mechanomicrobiology: How Bacteria Sense and Respond to Forces. *Nat. Rev. Microbiol.* **2020**, *18*, 227–240. [CrossRef] [PubMed]
40. Taylor, J.R. *An Introduction to Error Analysis*; University Science Books: Sausalito, CA, USA, 1997; 327p.
41. Keentok, M.; Xue, S.-C. Edge Fracture in Cone-Plate and Parallel Plate Flows. *Rheol. Acta* **1999**, *38*, 321–348. [CrossRef]
42. Mille, Y.; Beney, L.; Gervais, P. Viability of Escherichia Coli after Combined Osmotic and Thermal Treatment: A Plasma Membrane Implication. *Biochim. Biophys. Acta (BBA)-Biomembr.* **2002**, *1567*, 41–48. [CrossRef]
43. Sperandeo, P.; Martorana, A.M.; Polissi, A. Lipopolysaccharide Biosynthesis and Transport to the Outer Membrane of Gram-Negative Bacteria. *Bact. Cell Walls Membr.* **2019**, *92*, 9–37.
44. Hwang, H.; Paracini, N.; Parks, J.M.; Lakey, J.H.; Gumbart, J.C. Distribution of Mechanical Stress in the *Escherichia Coli* Cell Envelope. *Biochim. Biophys. Acta (BBA)-Biomembr.* **2018**, *1860*, 2566–2575. [CrossRef]
45. Xie, J.Y.; Ding, G.H.; Karttunen, M. Molecular Dynamics Simulations of Lipid Membranes with Lateral Force: Rupture and Dynamic Properties. *Biochim. Biophys. Acta (BBA)-Biomembr.* **2014**, *1838*, 994–1002. [CrossRef]
46. Gan, L.; Chen, S.; Jensen, G.J. Molecular Organization of Gram-Negative Peptidoglycan. *Proc. Natl. Acad. Sci. USA* **2008**, *105*, 18953–18957. [CrossRef]
47. Mitra, K.; Ubarretxena-Belandia, I.; Taguchi, T.; Warren, G.; Engelman, D.M. Modulation of the Bilayer Thickness of Exocytic Pathway Membranes by Membrane Proteins Rather than Cholesterol. *Proc. Natl. Acad. Sci. USA* **2004**, *101*, 4083–4088. [CrossRef]
48. Inouye, M. A Three-Dimensional Molecular Assembly Model of a Lipoprotein from the *Escherichia Coli* Outer Membrane. *Proc. Natl. Acad. Sci. USA* **1974**, *71*, 2396–2400. [CrossRef]
49. Willis, M.J.; Ahrens, T.J.; Bertani, L.E.; Nash, C.Z. Bugbuster—Survivability of Living Bacteria upon Shock Compression. *Earth Planet. Sci. Lett.* **2006**, *247*, 185–196. [CrossRef]
50. Faghih, M.M.; Sharp, M.K. Modeling and Prediction of Flow-Induced Hemolysis: A Review. *Biomech. Model. Mechanobiol.* **2019**, *18*, 845–881. [CrossRef] [PubMed]
51. Barthes-Biesel, D. Motion and Deformation of Elastic Capsules and Vesicles in Flow. *Annu. Rev. Fluid Mech.* **2016**, *48*, 25–52. [CrossRef]
52. Chang, K.-S.; Olbricht, W.L. Experimental Studies of the Deformation and Breakup of a Synthetic Capsule in Steady and Unsteady Simple Shear Flow. *J. Fluid Mech.* **1993**, *250*, 609–633. [CrossRef]
53. Lebedev, V.V.; Turitsyn, K.S.; Vergeles, S.S. Dynamics of Nearly Spherical Vesicles in an External Flow. *Phys. Rev. Lett.* **2007**, *99*, 218101. [CrossRef]
54. Deschamps, J.; Kantsler, V.; Steinberg, V. Phase Diagram of Single Vesicle Dynamical States in Shear Flow. *Phys. Rev. Lett.* **2009**, *102*, 118105. [CrossRef]
55. Semeraro, E.F.; Devos, J.M.; Porcar, L.; Forsyth, V.T.; Narayanan, T. In Vivo Analysis of the *Escherichia Coli* Ultrastructure by Small-Angle Scattering. *IUCrJ* **2017**, *4*, 751–757. [CrossRef]
56. Mullineaux, C.W.; Nenninger, A.; Ray, N.; Robinson, C. Diffusion of Green Fluorescent Protein in Three Cell Environments in Escherichia Coli. *J. Bacteriol.* **2006**, *188*, 3442–3448. [CrossRef]
57. Kelley, E.G.; Butler, P.D.; Ashkar, R.; Bradbury, R.; Nagao, M. Scaling Relationships for the Elastic Moduli and Viscosity of Mixed Lipid Membranes. *Proc. Natl. Acad. Sci. USA* **2020**, *117*, 23365–23373. [CrossRef]
58. Deng, Y.; Sun, M.; Shaevitz, J.W. Direct Measurement of Cell Wall Stress Stiffening and Turgor Pressure in Live Bacterial Cells. *Phys. Rev. Lett.* **2011**, *107*, 158101. [CrossRef]
59. Mathelié-Guinlet, M.; Asmar, A.T.; Collet, J.-F.; Dufrêne, Y.F. Lipoprotein Lpp Regulates the Mechanical Properties of the *E. Coli* Cell Envelope. *Nat. Commun.* **2020**, *11*, 1789. [CrossRef] [PubMed]
60. Garcia-Briones, M.A.; Chalmers, J.J. Flow Parameters Associated with Hydrodynamic Cell Injury. *Biotechnol. Bioeng.* **1994**, *44*, 1089–1098. [CrossRef] [PubMed]
61. Meneveau, C.; Sreenivasan, K.R. The Multifractal Nature of Turbulent Energy Dissipation. *J. Fluid Mech.* **1991**, *224*, 429–484. [CrossRef]